

# Stabilizing mechanism of the dipolar structure and its effects on formation of carriers in wurtzite {0001} films: InN and ZnO

Jung-Hwan Song,<sup>1</sup> Toru Akiyama,<sup>2</sup> and Arthur J. Freeman<sup>1,3</sup>

<sup>1</sup>*Department of Physics and Astronomy, Northwestern University, Evanston, Illinois 60208, USA*

<sup>2</sup>*Department of Physics Engineering, Mie University, Tsu 514-8507, Japan*

<sup>3</sup>*Department of Materials Science and Engineering, Northwestern University, Evanston, Illinois 60208, USA*

(Received 14 September 2007; published 31 January 2008)

The stabilization of the dipolar structure and its effects on carrier formation in wurtzite films are investigated through a case study of InN and ZnO {0001} films by means of the highly precise all-electron full-potential linearized augmented plane-wave method. The calculated total energies of both the wurtzite and graphitic structures demonstrate that the structural phase transition from the graphitic to wurtzite occurs when the thickness is beyond six (ten) bilayers in InN (ZnO). Our analysis of the calculated energies reveals that the phase transition is due to the competition between the bulk energy and the extra energy originating from the macroscopic electric field of the dipole structure. Further, an analysis of the electronic structure and charge densities in InN {0001} films reveals the screening role of the electric field. The screening effect causes a broadening of N  $2p$  states in the band structure by approximately 1.5 eV and charge redistribution in each polarizable unit. For InN and ZnO {0001} films, we have also found by using pseudohydrogens to passivate the opposite surfaces that the screening has little effect on the surface states and on the work functions. In contrast, the calculated formation energies of defects in InN {0001} films (N vacancy and substitutional Mg) using both pristine and pseudohydrogen passivated surfaces show that the internal electric field of the dipolar structure in wurtzite films may affect the formation of carriers near the surface. Thus, these results provide some fundamental characteristics for the polar surfaces of wurtzite films.

DOI: 10.1103/PhysRevB.77.035332

PACS number(s): 68.35.B-, 73.20.At, 81.10.Aj, 68.55.Ln

## I. INTRODUCTION

Nitrides and oxides with the wurtzite structure have been extensively studied for a broad range of nanoscale materials as possible optoelectronic devices due to a wide range of band gaps, and thus for possible band gap engineering by alloying with different elements.<sup>1,2</sup> Hence, it is important to understand the surface morphology and its physical properties. Interestingly, in experiments, many wurtzite films have polar surfaces, which indicates that the  $c$  axis ({0001}) is a natural growth orientation. In addition, the bonding of many wurtzite films such as ZnO shows strong ionic character. Hence, the epitaxial growth of wurtzite {0001} films has been an interesting problem due to the dipole structure, and thus the polar surfaces of the wurtzite materials. The physical properties for the polarity of the wurtzite {0001} films have been studied for several situations experimentally<sup>3,4</sup> and theoretically.<sup>4-6</sup> The fundamental problem of the wurtzite {0001} films is that, as the film thickness grows, the macroscopic electrostatic field due to the dipole structure may cause the surface (or cleavage) energy to diverge, which can make the system unstable.<sup>7</sup> However, the abundant formation of the {0001} surface morphology in experiments suggests that there must be a stabilizing mechanism in these films.

The stability problems of the polar surfaces have been visited already many times theoretically since Tasker's work in 1979.<sup>8</sup> The immediate solutions considered for stabilizing the wurtzite {0001} films would be surface reconstruction or the absorption of foreign atoms.<sup>8,9</sup> However, two other solutions have been proposed for the stabilizing mechanism of the pristine wurtzite films. One of them is the charge transfer mechanism from anion to cation surfaces, which makes the

cleavage energy converge as the film thickness increases;<sup>7</sup> the other is the structural phase transition observed for a very small number of wurtzite {0001} layers to the graphitic structure, which completely destroys the dipole structures.<sup>10</sup> This mechanism may play an important role in experiments. For instance, as the film thickness increases, the graphitic structure of the film at the initial deposition becomes unstable with respect to the wurtzite {0001} film, while the conversion energy to the nonpolar films is higher than that to the polar films.<sup>10</sup>

However, the physical mechanism of the screening of the dipolar electrostatic field and the relationship with the structural phase transition are still unclear, and the effects of polar surfaces and dipole structures on the physical properties with doping are barely known. To date, mainly Mulliken population analyses have been used as evidence of the charge transfer mechanism. Indeed, there are still open questions such as the participation of the system in the screening of the polar electric field and the effect of the screening on surface states at the Fermi level and on their work functions. The study of the clean polar surfaces is also essential to the understanding of the possible interaction between the internal electric field and surface reconstruction or role of substrates.

To answer these questions, we investigate the problems of the stabilizing mechanism with InN {0001} and ZnO {0001} films using a highly precise first-principles density functional approach. We also find that the screening may affect the formation of carriers due to the charge redistribution, for which we compare the formation energies of neutral defects (N vacancy and substitutional Mg) between the pristine and the pseudohydrogen passivated InN {0001} films. The internal electric field in six bilayers of InN {0001} films can cause

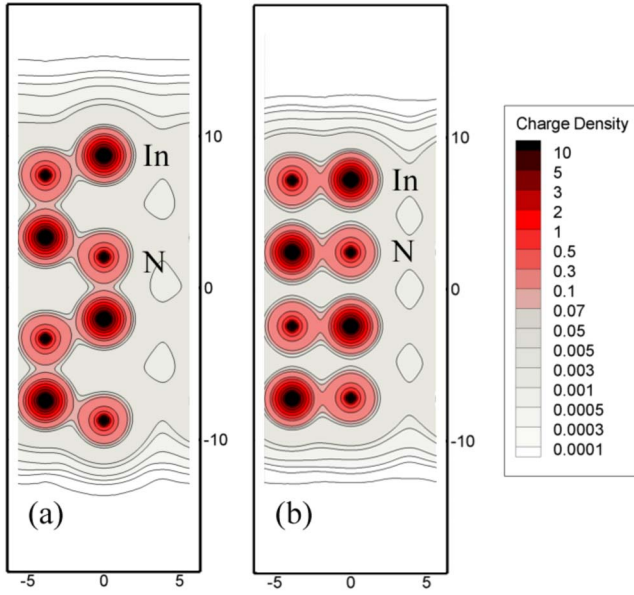


FIG. 1. (Color online) Cross sectional  $[11\bar{2}0]$  charge densities of (a) the fixed wurtzite structure and (b) the relaxed graphitic structure of four bilayers of InN  $\{0001\}$  films.

a lower formation energy for N vacancy by approximately 0.45 eV and a higher formation energy for Mg by approximately 0.19 eV.

## II. METHODOLOGY

The theoretical calculations were performed with the highly precise thin film all-electron full-potential linearized augmented plane-wave (FLAPW) method<sup>11,12</sup> within the local density approximation and the Hedin and Lundqvist exchange and correlation potential.<sup>13</sup> The thin film (single slab) FLAPW method has a fully two-dimensional geometry, and thus has no artificial three-dimensional periodicity as in superslab models which introduce vacuum regions between slabs. One advantage of this is that the work function is well defined, and two different work functions can be calculated at the same time for two different surfaces of the same slab such as wurtzite  $\{0001\}$  films and without worrying about the interaction between slabs. The  $k$  mesh in the Brillouin zone is  $13 \times 13$  for a  $1 \times 1$  unit cell, based on which the  $k$  mesh is changed for larger supercells accordingly. The energy cutoffs of the LAPW basis and the star functions are 13 and 144 Ry, which are used for the interstitial wave functions and for the charge density and potential, respectively. For the wurtzite structure, InN and ZnO  $\{0001\}$  films are calculated with up to 14 bilayers. For the graphitic structure, InN and ZnO films are calculated with up to four and eight layers, which correspond to four and eight bilayers of wurtzite structure, respectively.

## III. RESULTS AND DISCUSSION

### A. Structural phase transition and its mechanism

Like other wurtzite films such as GaN, AlN, and ZnO,<sup>10</sup> theoretical calculations show that polar  $\{0001\}$  films of InN

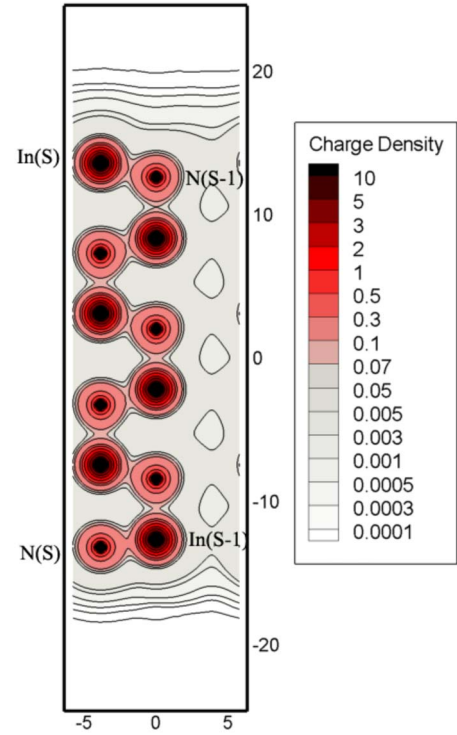


FIG. 2. (Color online) Charge densities of the relaxed structure of six bilayers of InN  $\{0001\}$  films. S and S-1 indicate the surface and subsurface layers, respectively.

with a small number of layers, for instance, two and four bilayers, have lower total energies for the graphitic relative to the wurtzite structure. As seen from these four bilayer InN  $\{0001\}$  FLAPW calculations, there are no significant charge densities between the layers in the graphitic structure, as shown in Fig. 1(b), while the covalent bonding character in Fig. 1(a) clearly shows the wurtzite structure. The FLAPW calculations for six bilayers of InN  $\{0001\}$  films, however, are lower in total energy and so maintain the wurtzite structure after the geometry optimization, as seen in Fig. 2.

Since there is a macroscopic electrostatic field due to the dipole structure of wurtzite  $\{0001\}$  films, those with a small number of layers must have lower total energies for the graphitic structures, that is, by removing the destabilizing dipoles. However, there is an additional energy cost since the graphitic structure has  $sp^2$  trigonal planar geometry, and hence has a higher bulk energy than the wurtzite structure. Now, if there is sufficient screening in such a way that the extra energy due to the extra electrostatic field is constant regardless of the thickness of the wurtzite  $\{0001\}$  films (that is, the cleavage energy converges), thicker graphitic films no longer have lower total energies due to the larger bulk energy. This may easily be seen if we employ the usual surface energy equations with the total energies of  $\{0001\}$  films of the wurtzite structure,  $E_W$ , and the graphitic structure,  $E_G$ . That is,

$$E_W = n\Delta E_{WB} + \Delta E_{elec,surf}^W,$$

$$E_G = n\Delta E_{GB} + \Delta E_{surf}^G, \quad (1)$$

where  $n$  is the number of bilayers,  $\Delta E_{WB}$  and  $\Delta E_{GB}$  are the bulk energies for a bilayer corresponding to each structure,  $\Delta E_{elec,surf}^W$  is the extra energy due to the electrostatic field and surfaces in the wurtzite structure, and  $\Delta E_{surf}^G$  is the extra energy due to the surfaces in the graphitic structure.

Now we may estimate the  $n_t$  at which InN {0001} films are stabilized in the wurtzite phase. For instance, if we use our calculated total energies for two and four bilayers to obtain the unknown variables  $\Delta E_{WB}$ ,  $\Delta E_{GB}$ ,  $\Delta E_{elec,surf}^W$ , and  $\Delta E_{surf}^G$ , then  $n_t$  can be solved for by using  $E_W(n_t) < E_G(n_t)$  in Eq. (1), and so

$$n_t > \frac{\Delta E_{surf}^G - \Delta E_{elec,surf}^W}{\Delta E_{WB} - \Delta E_{GB}}. \quad (2)$$

The bulk energy for the cleavage (or surface) energy calculations is usually determined from multiple film calculations so as to avoid the surface energy divergence with film thickness,<sup>14,15</sup>

$$\Delta E_{WB} = E_W(m) - E_W(m-1),$$

$$\Delta E_{GB} = E_G(m) - E_G(m-1), \quad (3)$$

where  $m$  is the number of layers, and one should check the convergence of the bulk energy as  $m$  increases.

In addition, even the bulk energy in the clean wurtzite {0001} films must be different from that of the wurtzite bulk system mainly due to the electric field of the dipole structure and the screening.<sup>23</sup> In order to avoid any ambiguity, we have simply compared the total energies (per  $1 \times 1$  unit cell) of the two structures as in Fig. 3(a), and have estimated  $n_t$  using Eq. (2) to see how  $n_t$  converges, as in Fig. 3(b). Now,  $E_{elec,surf}^W$  and  $E_{surf}^G$  are not constants and converge as the film thickness increases, while  $E_{WB}$  and  $E_{GB}$  are constants. Hence, the total energy difference in Fig. 3(a) does not show a linear behavior. Also note in Eqs. (1) and (2) that  $E_{elec,surf}^W$  is larger than  $E_{surf}^G$ , and that, as explained earlier,  $E_{GB}$  is larger than  $E_{WB}$ , which leads to positive  $n_t$  values in Fig. 3(b).

The  $n_t$  estimated by Eq. (2) in Fig. 3(b) indicates that the geometry optimization calculations show that the ZnO {0001} films with ten bilayers are stable in the wurtzite structure. We have confirmed this result by performing the geometry optimization for ten bilayers of ZnO, as found previously.<sup>10</sup> Very interestingly, the estimated  $n_t$  in Fig. 3(b) rapidly converges as the film thickness increases, which suggests that the interaction between the surfaces quickly becomes negligible and, more importantly, that the extra energy due to the dipole structure also rapidly converges due to the screening. This was easily confirmed by calculations of the potential energy differences between cation and anion surface layers of wurtzite films. Figure 4(a) illustrates the potential energy along the  $c$  axis of InN {0001} films; films which are thicker than four bilayers do not show any significant variation in the potential energy difference between the anion and cation surfaces. The first derivative of the potential with respect to the distance in Figs. 4(a) and 4(b) shows that the contribution from the surface region is relatively large compared to that at the central bilayers as the film thickness

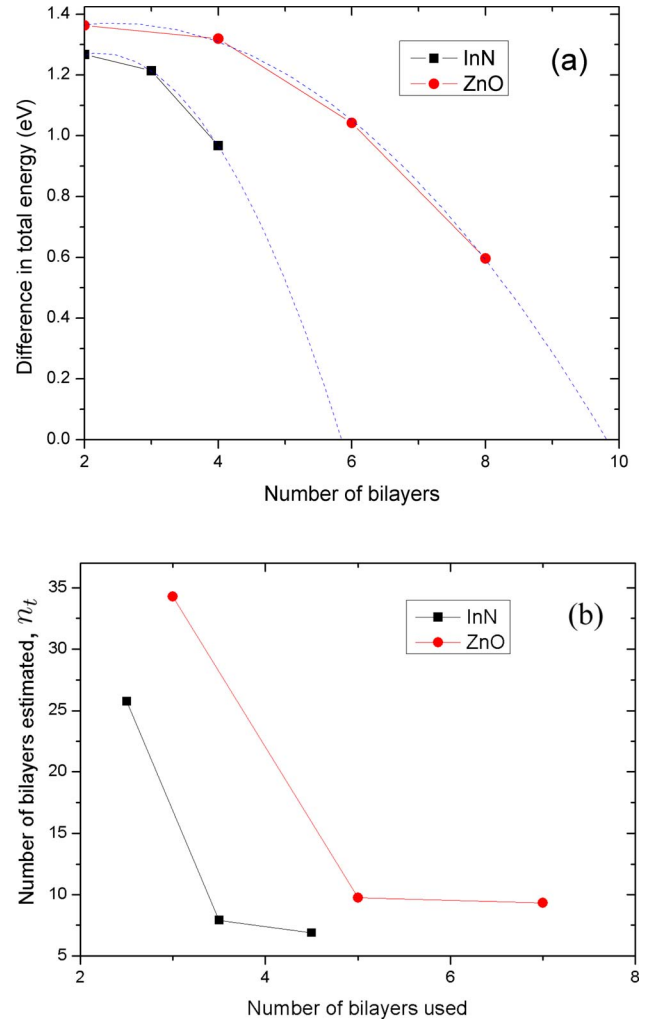


FIG. 3. (Color online) (a) Total energy differences,  $E_W - E_G$ , between wurtzite and graphitic structures for InN and ZnO as a function of the number of bilayers. The data points are fitted by a parabolic function. (b) The number of bilayers,  $n_t$ , which is estimated using Eq. (2). The  $x$  axis in (b) indicates the average number of bilayers used to solve for variables such as  $\Delta E_{WB}$ ,  $\Delta E_{GB}$ ,  $\Delta E_{elec,surf}^W$  and  $\Delta E_{surf}^G$  in Eq. (1).

increases. Figure 4(b) shows very similar behavior of ZnO films. However, the potential energy difference in ZnO films is larger by approximately 1.2 eV compared to that in InN films due to the larger ionicity of ZnO.

Figure 4(c) demonstrates that InN and ZnO {0001} films indeed have the quickly converging potential energy difference as a function of the film thickness due to the screening in the wurtzite structure, which makes the cleavage (surface) energy converge as the film thickness increases. Now, the additional bulk energy,  $\Delta E_{GB} - \Delta E_{WB}$ , increases in proportion to the number of bilayers, which causes the system for a certain thickness to maintain the wurtzite structure during the geometry optimization, as one can notice in Eq. (2). One difficulty in this analysis, however, is that it is not always possible to separate the relaxed wurtzite structure into the  $sp^2$  graphitic and  $sp^3$  wurtzite structures. For example, in five bilayer InN films, the surface bilayers almost completely collapse to the graphitic structure by the geometry optimization,

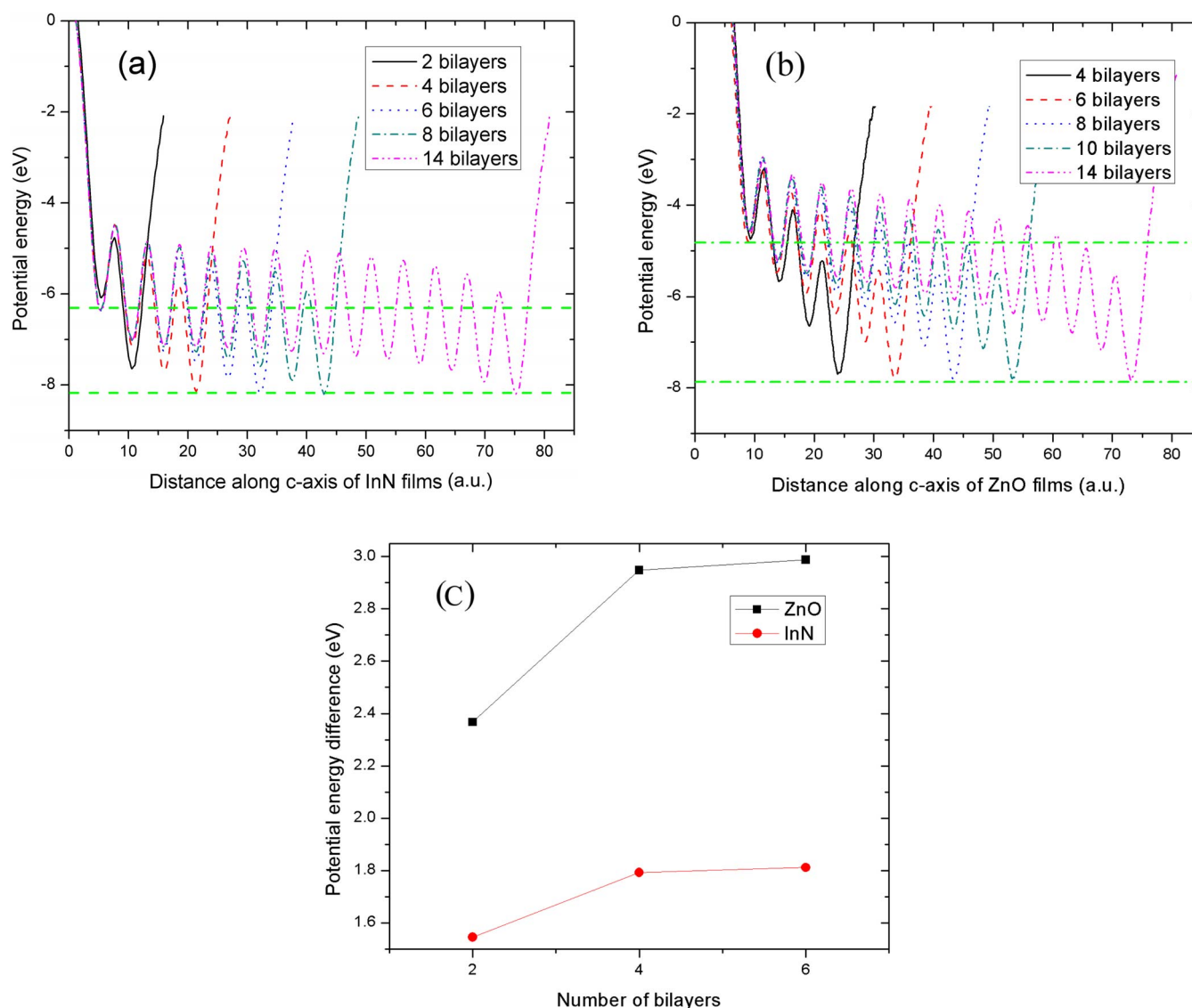


FIG. 4. (Color online) (a) Potential energy along the  $c$  axis at the same in-plane coordinates of the InN {0001} films. The dashed horizontal lines are guides to the eye. The upper and lower horizontal lines indicate the potential energies at the anion surface and the cation surface, respectively. (b) Potential energy along the  $c$  axis at the same in-plane coordinates of the ZnO {0001} films. (c) Potential energy difference between the anion and the cation surfaces for different numbers of bilayers of InN and ZnO {0001} films (wurtzite structure).

and thus show the  $sp^2$  geometry. However, the distance along the  $c$  axis between the cation and the anion center layers is reduced by only about 30%, and so the central bilayers maintain the  $sp^3$  geometry.

### B. Screening of the dipolar electrostatic field

The screening which causes the extra energy due to the dipole structure to converge can be seen from an analysis of the electronic structure. While the band structure of the graphitic structure shows insulating behavior in four bilayer InN {0001} films in Fig. 5(a), which indicates that there are no dangling bonds, the band structure of the pristine six bilayers of wurtzite InN {0001} films shows the effect of screening compared to the bulk band structure as in Fig. 5(b). For instance, Fig. 5(b) demonstrates that the lowest energy level of the N  $2p$  state at  $\bar{M}$  in the band structure of InN {0001}

films is lower than that of InN bulk by approximately 1.5 eV. The broadening of the bands indicates that the charge distribution is significantly changed in the InN {0001} films compared to that in the bulk system. As one can see, in the pristine wurtzite {0001} film, the charge transfer mechanism can be explained as the screening of the extra electric field.

More specifically, in order to identify the screening of the macroscopic electrostatic field, we have calculated the difference in the charge densities between the clean InN {0001} films and the bulk InN system, which can then be considered as the effective induced charges due to the extra electric field. Now, the charge differences around the surfaces in Fig. 6 are not useful due to subtraction of the bulk charge from the charge around the surface region. Remarkably, Fig. 6 does show features in the induced charges around the N atoms in the central regions and, notably, that every atom (especially N atoms due to their ionic character) contributes to



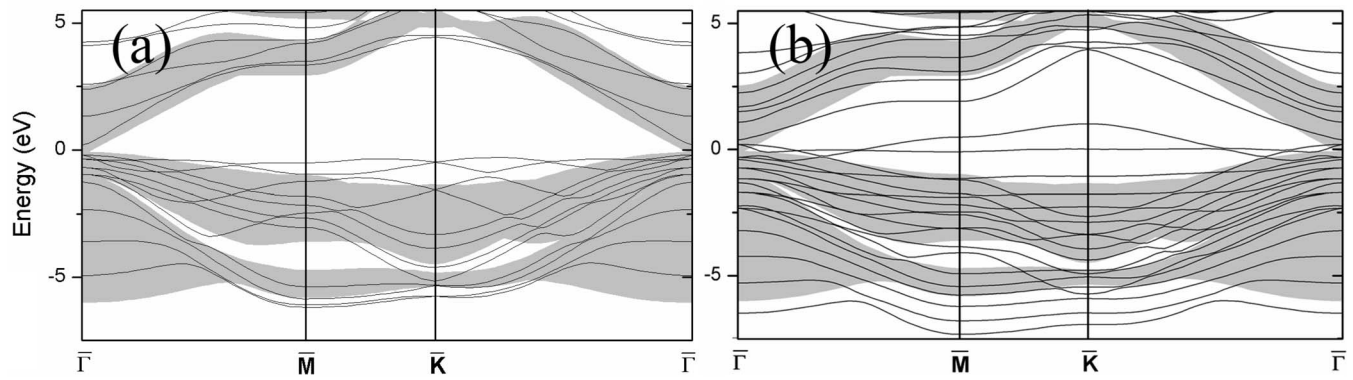


FIG. 5. Band structures of the relaxed structure of (a) graphitic four bilayers and (b) wurtzite six bilayers of InN {0001} films. The gray area is the bulk band structure which is projected onto the film geometry.

the screening and behaves as if there is an external electric field.<sup>16</sup> Indeed, the screening response of ionic materials such as LiCl in an external electric field can be found,<sup>16</sup> which shows the repeating ( $\pm$ ) sign behavior of the induced charges along the  $c$  axis around anion atoms, i.e., just as in the pristine InN {0001} films in this work. This appears to be due to the charge transfer through the maximum peak of the valence charge density, as indicated in Ref. 16.

As one can see in Fig. 6, the charge transfer occurs mainly for each polarizable unit (in this case, mainly anion atoms) and, thus, the Mulliken population analyses are not sufficient for the interpretation of the screening. Now, while Wander *et al.*<sup>7</sup> argued that the change in ionicity is highly localized around the surface region and decays to zero by the third bilayer below the surface layer even in ZnO {0001} films, our

study shows that the screening is a considerably longer ranged interaction. For example, the polarizable units in all 14 bilayers of InN {0001} films contribute to the screening, as shown in Fig. 6. In particular, the surface region is largely affected by the screening, as in Fig. 4(a), and the effect on the central bulk layers becomes negligibly small as the film thickness increases, as in Fig. 6.

### C. Effect of screening on surface states and work functions

To date, it is believed that the metallic states (surface states around the Fermi level,  $E_F$ ) are caused by the charge transfer mechanism.<sup>7,10</sup> This speculation, however, does not consider dangling bonds and surface states properly. In general, surface states exist near  $E_F$  due to their nonbonding

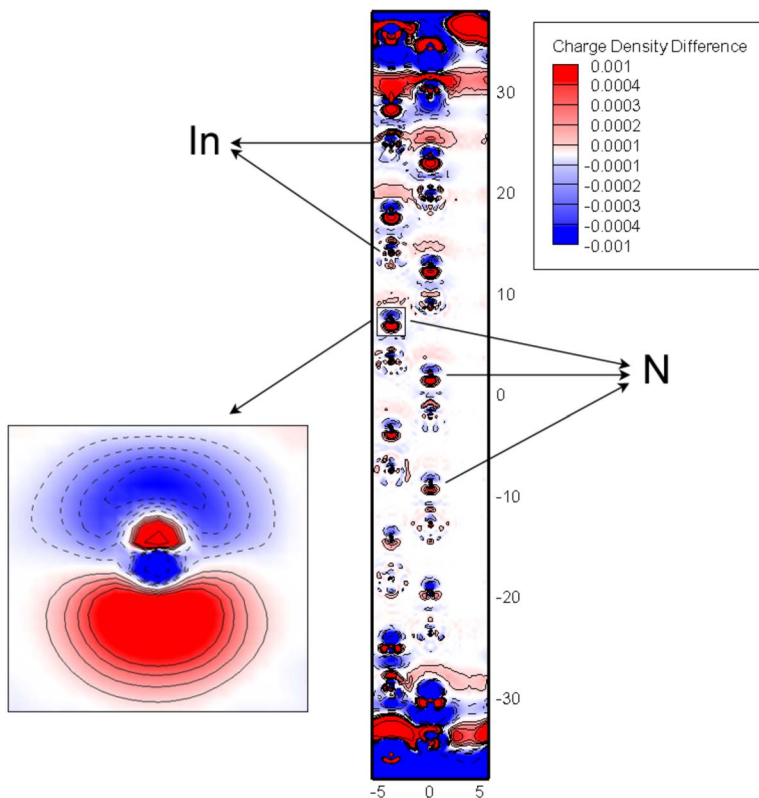


FIG. 6. (Color online) The difference in the charge densities between bulk InN and clean InN {0001} film shows here that even the central layers in 14 bilayers are affected by the screening; the enlarged N contour plot to the left details some of these results. The solid and dashed lines indicate positive and negative values, respectively.

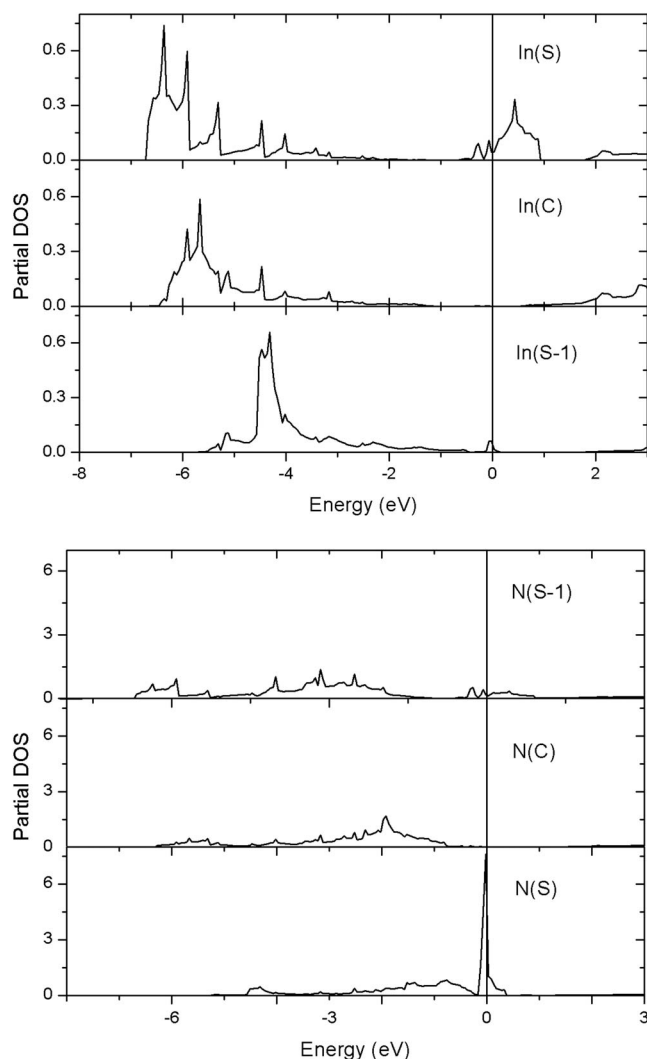


FIG. 7. Layer-resolved density of states projected onto In  $s$  and N  $p$  states in a six bilayer wurtzite InN {0001} film. S, C, and S-1 indicate the surface, central, and subsurface layers, respectively. In(S) and N(S-1) denote the (0001) surface layers, and In(S-1) and N(S) denote the (000 $\bar{1}$ ) surface layers.

character<sup>17,18</sup> and the charge distribution near the surface is distorted due to the broken translational symmetry and the vacuum. Now, Figs. 7 and 8 clearly demonstrate that the surface states in wurtzite {0001} films such as InN and ZnO indeed occur near the band gap as a relatively large density of states. The cation surface states in both InN and ZnO films are relatively dispersive near the conduction band minimum compared to the narrow peaks of the anion surface states near the top of the valence band. A comparison of cation  $s$  and anion  $p$  states in Figs. 7 and 8 between the surface and the central layers shows not only the pronounced surface states at  $E_F$  but also the shifting character of density of states peaks, which is consistent with the potential drop in Fig. 4. To see whether the metallic surface states are really related to the charge transfer mechanism and to understand the effect of the screening on surface states at  $E_F$ , we have employed pseudohydrogens with a noninteger core charge<sup>19</sup> to passivate the InN {0001} films and have compared band structures

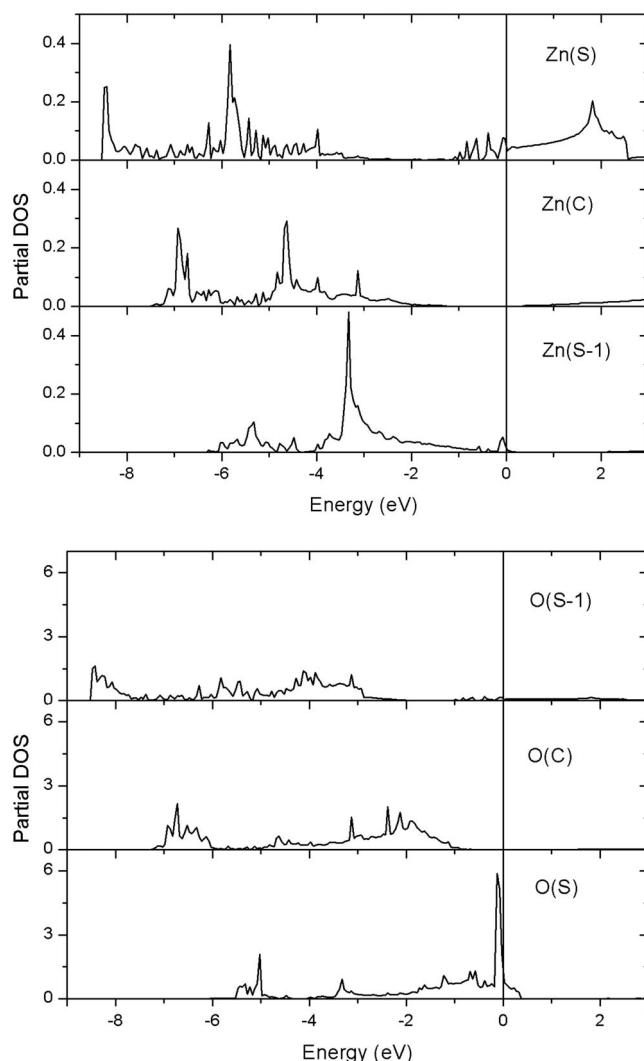


FIG. 8. Layer-resolved density of states projected onto Zn  $s$  and O  $p$  states in a ten bilayer wurtzite ZnO {0001} film. S, C, and S-1 indicate the surface, central, and subsurface layers, respectively. Zn(S) and O(S-1) denote the (0001) surface layers, and Zn(S-1) and O(S) denote the (000 $\bar{1}$ ) surface layers.

for six bilayer films (see Fig. 9) passivated with 1.25 and 0.75 pseudohydrogen charges for the N and In surface layers, respectively. As is well known, the pseudohydrogens are usually used to remove undesirable surface states and to remove the interaction between surfaces so as to reduce the computational cost by decreasing the number of layers. In addition, we have found that the pseudohydrogens also significantly reduce the extra electrostatic field in the wurtzite films. In Fig. 9, we show that the band structure of the passivated InN {0001} films with pseudohydrogens indeed coincides very well with the bulk band structure (projected onto the film geometry).

To study the surface states of the polar surface films, we have passivated only one surface at a time, that is, either the In surface or N surface, to compare with both N and In terminated clean surfaces of InN films. For instance, in Fig. 10(b), only the N surface is passivated with pseudohydrogens to study In surface states at  $E_F$ . This polar surface study

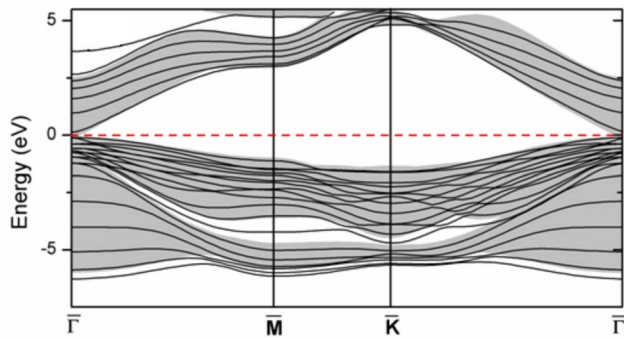


FIG. 9. (Color online) Band structure of six bilayers of wurtzite InN {0001} films passivated with pseudohydrogens. The gray area is the bulk band structure which is projected onto the film geometry.

is based on the fact that even when only one surface is passivated with pseudohydrogens, the band structure (except surface states) is similar to the bulk band structure, which suggests that the extra electric field due to the dipole structure is significantly reduced. Indeed, as can be seen in Figs. 10(a) and 10(b), we have found that the unoccupied In surface states at  $E_F$  remain exactly the same when the N surface states are moved away from  $E_F$  due to the passivation. The same explanation applies to the N surface when only the In surface is passivated, as in Fig. 10(c). This pseudohydrogen passivation study suggests that the metallization in the band structure of the pristine {0001} films with wurtzite structure has little relationship with the charge transfer mechanism or the screening and is simply due to the lack of electrons or dangling bonds at the surfaces. One possible problem here is that density functional calculations within local density approximation (LDA) for bulk InN yield a nearly zero band gap, which might affect the results.<sup>20</sup> However, our band structure calculations show no overlap between valence and conduction bands and, more importantly, no electron occupancy in the conduction bands.

We note that it is also difficult to make any further analysis of the screening in wurtzite {0001} films using a simple model such as the *bulk* band structure due to the dominant surface states, different band gaps of film structures, and possible Fermi alignments.<sup>21</sup> Thus, we performed calculations using the same pseudohydrogen methodology for ten bilayer ZnO films to confirm our conclusions.<sup>24</sup> Note that density functional calculations with LDA show a roughly 0.8 eV band gap for bulk ZnO. Now, the results for ZnO {0001} films in Figs. 11(a)–11(c) show the same behavior as for the InN films. The surface states are hardly affected by the opposite surface passivation with pseudohydrogens, while the valence bands dramatically change in Figs. 11(b) and 11(c) compared to the clean surface case in Fig. 11(a). One can notice the small occupation near  $\Gamma$  in Figs. 10(b) and 11(b). We have found that this is an artificial occupation due to the artificial pseudohydrogens. Further, this occupation can be changed by using different pseudohydrogen charges, while the Zn surface states are again not affected by different pseudohydrogen charges, and thus possibly different screenings. Thus, these calculations from the narrow (InN) to the wide (ZnO) band gap materials confirm that metallic surface

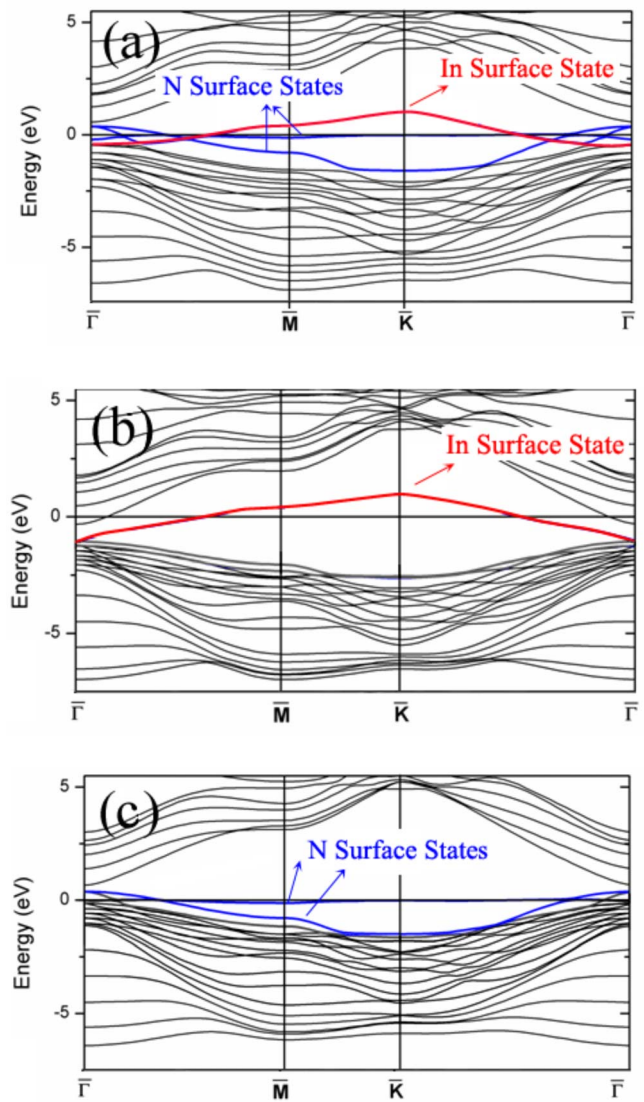


FIG. 10. (Color online) Band structures of wurtzite six bilayers of (a) a pristine InN {0001} film, (b) the InN {0001} film with the opposite N surface layer passivated with pseudohydrogens, and (c) the InN {0001} film with the opposite In surface layer passivated with pseudohydrogens. N surface states in (b) and In surface states in (c) were moved away from  $E_F$  by the passivation. The surface states in (b) and (c) remain the same when the opposite surface is pseudohydrogen passivated.

states are caused mainly by the surface discontinuation of the bulk (e.g., broken translational symmetry and dangling bonds).

The work function calculations show consistent behavior: No significant change in the work function of the In surface is found when only the N surface is passivated. Indeed, the calculations show only 1% and 0.1% differences in the work function for the In and the N surfaces, respectively, when the opposite polar surface is passivated. The work function directly reflects the change in the surface states around  $E_F$  or the surface structure. For instance, as shown in Table I, the work function calculations yield 3.79 eV for the cation surface and 6.32 eV for the anion surface of six bilayers of the



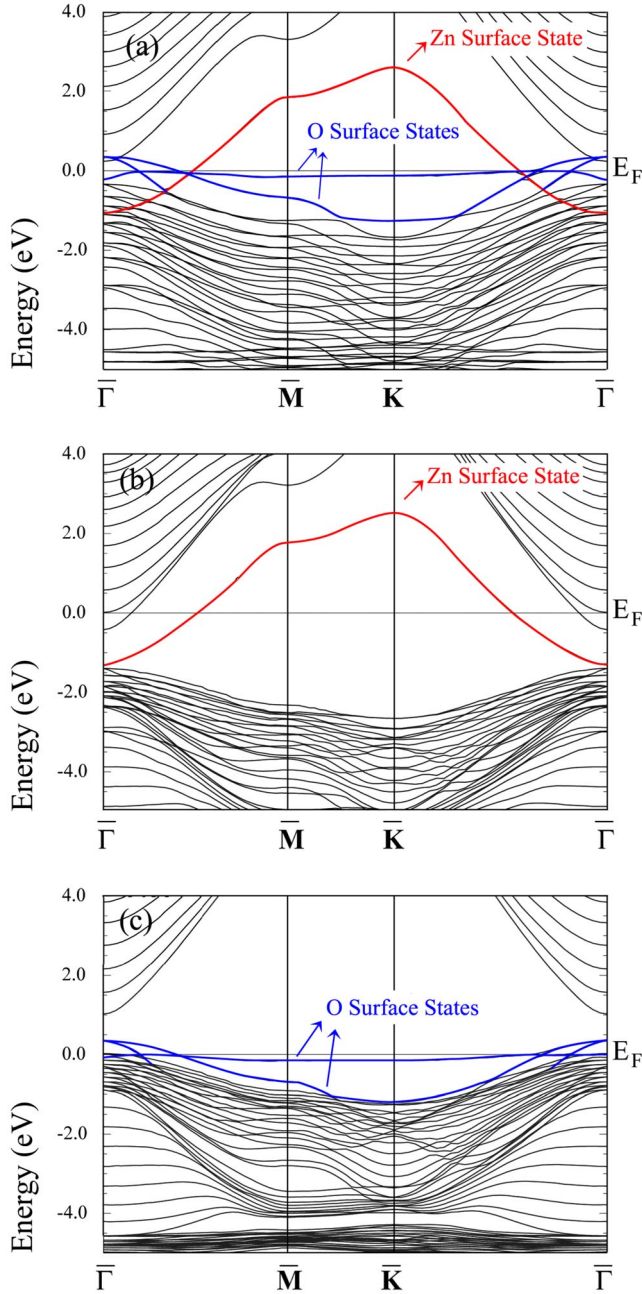


FIG. 11. (Color online) Band structures of wurtzite ten bilayers of (a) a pristine ZnO {0001} film, (b) the ZnO {0001} film with the opposite O surface layer passivated with pseudohydrogens, and (c) the ZnO {0001} film with the opposite Zn surface layer passivated with pseudohydrogens. O surface states in (b) and Zn surface states in (c) were moved away from  $E_F$  by the passivation. The surface states in (b) and (c) remain the same when the opposite surface is pseudohydrogen passivated as in the InN film case.

relaxed pristine InN {0001} films. In two and four bilayers of wurtzite InN {0001} films, the difference in work function due to the two different polar [(0001)/(000 $\bar{1}$ )] surfaces, however, disappears (as in Table I) after the structural relaxation to the graphitic structure which has no destabilizing dipoles. The work functions of the graphitic structure in two

TABLE I. Work functions for two, four, and six bilayers of InN {0001} films.

No. of bilayers	Nonrelaxed (wurtzite) (eV)	Relaxed (eV)
2	Cation surface: 3.24 Anion surface: 7.11	Surface 1: 4.67 Surface 2: 4.67
4	Cation surface: 4.02 Anion surface: 7.47	Surface 1: 4.75 Surface 2: 4.73
6	Cation surface: 4.04 Anion surface: 7.42	Cation surface: 3.79 Anion surface: 6.32

and four bilayers of InN {0001} films are approximately 4.7 eV for both surfaces.

#### D. Effect of screening on the formation of carriers

Although the internal dipolar electric field has little effect on the surface states at  $E_F$ , defects and impurities near the surface region may be affected not only by surface states but also by the internal electric field or the charge redistribution caused by the screening. To show the effect of the internal electric field for neutral defects, we have compared the formation energies<sup>22</sup> of N vacancy ( $n$  type) and Mg doping ( $p$  type) at the central layer of six bilayers between the two different InN {0001} films: the first with clean In and N surfaces and the second with a clean In surface and with the opposite N surface passivated with pseudohydrogens.<sup>25,26</sup> The relevant chemical potentials are assumed to be the same between the two systems. We found that the second system, in which the electric field is greatly reduced by passivation of the N surface, as explained above in Sec. III C, has a higher formation energy for a N vacancy by approximately 0.45 eV and a lower formation energy for Mg by approximately 0.19 eV. This difference between the  $n$ -type and  $p$ -type carriers is envisioned to be related to the screening mechanism. As shown above in Sec. III B, the screening occurs by the charge (electron) transfer in the main polarizable units (anions). The extra electrons due to the N vacancy may efficiently screen the internal electric field, which yields a much lower total energy compared to the reference system (pristine {0001} film), while the holes due to Mg doping as a substitution of In cannot help the screening on the anion atom sites. These calculated results show that different strategies for efficient carrier generation, which depend on the carrier type especially near the surface, may be necessary, such as controlling the internal electric field which may be reduced by surface reconstructions or passivations.

#### IV. SUMMARY AND CONCLUSIONS

We have shown, by the highly precise thin film FLAPW method, that the structural phase transition from the graphitic to the wurtzite structure with increasing thickness can be accounted for mainly by the competition between the additional bulk energy due to the structural difference and the



extra energy due to the macroscopic electric field of the dipole structure. We have demonstrated that the cleavage energy of the InN and ZnO {0001} films in the wurtzite structure converges quickly due to the screening as the film thickness increases. This screening effect causes the charge redistribution in the system and the broadening of the band structure. On the other hand, the screening has little effect on surface states at the Fermi level, and thus on the work functions. Finally, the internal electric field of the dipolar struc-

ture in wurtzite {0001} films may affect the formation of carriers near the surface due to its stabilizing mechanism.

### ACKNOWLEDGMENTS

This work was supported by the NSF through its MRSEC program at the Materials Research Center of Northwestern University and by NREL (Grant No. DE-AC36-98GO103).

- 
- <sup>1</sup>H.-C. Hsu, C.-Y. Wu, H.-M. Cheng, and W.-F. Hsieh, *Appl. Phys. Lett.* **89**, 013101 (2006).  
<sup>2</sup>W. Walukiewicz, S. Li, J. Wu, K. Yu, J. A. III, E. Haller, H. Lu, and W. J. Schaff, *J. Cryst. Growth* **269**, 119 (2004).  
<sup>3</sup>T. Sasaki and T. Matsuoka, *J. Appl. Phys.* **64**, 4531 (1988).  
<sup>4</sup>V. K. Lazarov, J. Zimmerman, S. H. Cheung, L. Li, M. Weinert, and M. Gajdardziska-Josifovska, *Phys. Rev. Lett.* **94**, 216101 (2005).  
<sup>5</sup>R. B. Capaz, H. Lim, and J. D. Joannopoulos, *Phys. Rev. B* **51**, 17755 (1995).  
<sup>6</sup>C. Bungaro, K. Rapcewicz, and J. Bernholc, *Phys. Rev. B* **59**, 9771 (1999).  
<sup>7</sup>A. Wander, F. Schedin, P. Steadman, A. Norris, R. McGrath, T. S. Turner, G. Thornton, and N. M. Harrison, *Phys. Rev. Lett.* **86**, 3811 (2001).  
<sup>8</sup>P. W. Tasker, *J. Phys. C* **12**, 4977 (1979).  
<sup>9</sup>C. Noguera, *J. Phys.: Condens. Matter* **12**, R367 (2000).  
<sup>10</sup>C. L. Freeman, F. Claeysens, N. L. Allan, and J. H. Harding, *Phys. Rev. Lett.* **96**, 066102 (2006).  
<sup>11</sup>E. Wimmer, H. Krakauer, M. Weinert, and A. J. Freeman, *Phys. Rev. B* **24**, 864 (1981).  
<sup>12</sup>H. J. F. Jansen and A. J. Freeman, *Phys. Rev. B* **30**, 561 (1984).  
<sup>13</sup>L. Hedin and B. I. Lundqvist, *J. Phys. C* **4**, 2064 (1971).  
<sup>14</sup>C. Ruberto, Y. Yourdshahyan, and B. I. Lundqvist, *Phys. Rev. B* **67**, 195412 (2003).  
<sup>15</sup>V. Fiorentini and M. Methfessel, *J. Phys.: Condens. Matter* **8**, 6525 (1996).  
<sup>16</sup>M. S. Hybertsen and S. G. Louie, *Phys. Rev. B* **35**, 5602 (1987).  
<sup>17</sup>W. Shockley, *Phys. Rev.* **56**, 317 (1939).  
<sup>18</sup>M. Posternak, H. Krakauer, A. J. Freeman, and D. D. Koelling, *Phys. Rev. B* **21**, 5601 (1980).  
<sup>19</sup>K. Shiraiishi, *J. Phys. Soc. Jpn.* **59**, 3455 (1990).  
<sup>20</sup>B. Meyer and D. Marx, *Phys. Rev. B* **67**, 035403 (2003).  
<sup>21</sup>G. Kresse, O. Dulub, and U. Diebold, *Phys. Rev. B* **68**, 245409 (2003).  
<sup>22</sup>C. Stampfl, C. G. Van de Walle, D. Vogel, P. Kruger, and J. Pollmann, *Phys. Rev. B* **61**, R7846 (2000).  
<sup>23</sup>A cleavage energy comparison between the wurtzite and graphitic structures was performed in Ref. 10, where they subtracted wurtzite bulk energies regardless of the structure. This causes an ambiguity.  
<sup>24</sup>Note that the ZnO {0001} films and InN {0001} films in the wurtzite structure which are thicker than ten and six bilayers, respectively, do not collapse to the graphitic structure by the geometry optimization.  
<sup>25</sup>The reason why the bulk system is not used for the comparison of formation energies is that the In surface layer may significantly interact with impurities at the center layer of six bilayer InN {0001} films. In this case, the interaction between the In surface layer and impurities in both terminated systems should be allowed. On the other hand, we found that the charge distribution of the N surface layer around  $E_F$  is localized well.  
<sup>26</sup>In these calculations, only the central four bilayers are relaxed to see the effect of only the internal electric field.